JOINT EUROPEAN TORUS JET

JET–P(89)29

J.A. Heikkinen, K. Avinash
and JET Team

Nonlinear Power Conversion During ICRF Heating at the Plasma Edge

Nonlinear Power Conversion During ICRF Heating at the Plasma Edge

J.A. Heikkinen[1], K. Avinash[2]
and JET Team*

JET-Joint Undertaking, Culham Science Centre, OX14 3DB, Abingdon, UK

[1]Technical Research Centre of Finland, Nuclear Engineering Laboratory, P.O. Box 169, SF-00181, Helsinki, Finland
+Institute of Plasma Research, Bhat Gandhinagar 382424, Gujrat, India
** See Appendix 1*

Preprint of Paper to be submitted for publication in
Nuclear Fusion

NONLINEAR POWER CONVERSION DURING ICRF HEATING AT THE PLASMA EDGE

J.A. Heikkinen* and K. Avinash‡

JET Joint Undertaking, Abingdon, Oxon. OX14 3EA, U.K.

ABSTRACT

The parametric decay of the fast magnetosonic wave to an ion Bernstein wave and a quasimode is analysed to estimate the amount of power converted nonlinearly at the plasma edge during ion cyclotron heating. Low decay thresholds for the pump wave amplitude are obtained when the quasimode frequency is at the hydrogen cyclotron frequency and the fast wave frequency is near appropriate cyclotron harmonics (or their sums) of the edge plasma. To obtain an upper limit for the growth of the decay modes nonlinear Landau damping of the Bernstein wave as a secondary process, in addition to the usual convective and linear damping processes of the decay waves, is studied. It is shown that due to the secondary process and finite interaction geometry in the decay a negligible power conversion from the fast wave to Bernstein modes may follow even if the pump wave amplitude clearly exceeds the threshold. At larger pump wave fields (>200 V/cm) a non-negligible power conversion could be obtained in spite of saturation of the instability. Because the wave fields of the fast wave at the plasma edge of JET tokamak are estimated to be less than 200 V/cm no serious power losses for the heating wave due to the Bernstein wave decay at the edge are expected. This seems to be in accordance with the recent observations in JET. These dependences are described and applications to H-minority heating of deuterium and deuterium-tritium plasma by ICRF waves in JET are presented.

*Technical Research Centre of Finland, Nuclear Engineering Laboratory
P.O. Box 169, SF-00181, Helsinki, Finland.
‡Institute of Plasma Research, Bhat Gandhinagar 382424, Gujrat, India

1. INTRODUCTION

There is wide experimental evidence that parametric instabilities may affect the power deposition in different wave heating schemes. Various decay processes may cause anomalous absorption of the heating wave which may be deleterious or beneficial depending on the spatial location of the instability. During intense ICRF heating by fast magnetosonic wave, the decay of the fast wave into an ion Bernstein wave and an ion quasimode has been theoretically predicted [1-5] and has been observed in the scrape-off layer in tokamaks [4,12]. It has been proposed [4,12] that the direct edge heating and consequent enhancement of density and impurity production in some ICRF heating experiments could be due to this decay. Recently, however, no clear connection between these deleterious phenomena and the fast wave decay to Bernstein modes was found in JET [13]. In an earlier study [5] the possibility of this decay at the plasma periphery during typical ICRF heating scenarios was investigated and low thresholds typically < 100 V/cm were obtained.

In this work we extend this study further. In particular we improve upon the estimates of the threshold presented earlier for the decay process in D-H plasmas by including proper geometrical effects. In addition, we also present estimates of the threshold for this decay in deuterium-tritium-hydrogen (D-T-H) plasma which is of great relevance to future experiments. Finally we evaluate the amount of power conversion from the fast wave to the decay waves as a function of relevant parameters. This power depends on the coupling geometry, the electric field of the fast wave and on the noise level of the decay waves. Generally, the calculations regarding converted power are complicated due to the nonlinear nature of the instability and different damping mechanisms of the decay waves. The decay waves may experience the collisional damping, the usual Landau damping, cyclotron damping or convective damping due to the finite interaction region. The nonlinear wave particle

interactions, secondary decay processes, pump depletion etc. also strongly affect the power conversion provided the decay waves attain a large amplitude. Since in the experiments the amplitudes of the decay waves at the edge have been observed to be small [2,4] [at most 10-15% of the total coupled power is attributed to the direct edge heating], we neglect pump depletion effects. To obtain an upper limit on the power conversion at the edge, we consider the secondary decay process of the Bernstein wave into another Bernstein wave and an electron quasi-mode.

Without any saturation of the instability the decay wave amplitudes would grow exponentially according to the $\exp(aE_o^2L)$ dependence where a is some constant depending on plasma parameters, E_o the fast wave field amplitude and L the growth length. With a sufficiently large E_o the power converted from the fast wave to the decay waves would be essential and the effect of the reduction of E_o should be considered. However, the secondary decay process is able to quench the exponential growth of the decay modes and, consequently, the power conversion from the fast wave may remain small provided the daughter modes in the secondary decay do not couple back to the fast wave. The secondary decay process presented in this paper is the well-known nonlinear electron Landau damping of Bernstein waves and involves the transfer of energy from long to short wavelengths. Although the frequency width in the spectrum remains small, it is large enough to decouple the main part of the secondary modes from the fast wave. Instead of solving the usual weak turbulence kinetic equation for the whole spectrum we demonstrate the strength of the secondary process by inspecting the coupling of two properly chosen resonant Bernstein waves. The description turns out to be a good approximation due to the frequency and wavenumber dependences of the Bernstein wave damping and growth.

The results of this paper show the importance of the saturation mechanism and one may find a negligible power conversion from the fast wave to the

Bernstein modes with E_o clearly exceeding the threshold but not being too large with typical tokamak edge parameters. Proper geometric effects on both the primary and secondary decay are included to obtain sufficiently realistic results. Special effort is also put to find the most dangerous (i.e. having the lowest threshold) primary decays from the various possible decay processes in different heating scenarios. The numerical results are given only for these special cases.

The plan of the paper is as follows. The main characteristics of the decay are reviewed in Section 2, and the saturation model of the instability is presented in Section 3. The method to evaluate the power conversion is explained in Section 4. Section 5 deals with estimates of power conversion in typical heating scenarios while in the last section we have discussed and summarised our results.

2. NON-RESONANT BERNSTEIN WAVE DECAY OF THE FAST WAVE

The decay of fast magnetosonic wave with frequency ω_o and a wave number $\vec{k}_o$ to ion Bernstein waves obeys the energy and momentum conservation rules which are

$$\omega_o = \omega_B + \omega, \qquad \vec{k}_o = \vec{k}_B + \vec{k}. \tag{1}$$

The frequency and wave numbers of the resonant Bernstein mode are denoted by ω_B and $\vec{k}_B$, while those of the non-resonant mode, called the quasimode, are denoted by ω and $\vec{k}$, respectively. The dielectric function of the ion Bernstein wave in a multi-ion species plasma is given by

$$\epsilon(\omega,\vec{k}) \equiv 1 + \chi_e(\omega,\vec{k}) + \sum_\delta \chi_\delta(\omega,\vec{k}) \ . \tag{2}$$

Here χ_e and χ_δ, which are the susceptibilities of the electrons and ion species δ respectively, are defined as

$$\chi_e(\omega,\vec{k}) = \frac{\omega_{pe}^2}{k^2 v_e^2}\left[1 + \frac{\omega}{k_z v_e} Z(\frac{\omega}{k_z v_e})\right] , \tag{3}$$

$$\chi_\delta(\omega,\vec{k}) = \frac{\omega_{p\delta}^2}{k^2 v_\delta^2} \frac{1 + \sum_{m=-\infty}^{\infty} \Lambda_m(b_\delta) \frac{\omega + i\nu_\delta}{k_z v_\delta} Z(\frac{\omega + i\nu_\delta - m\Omega_\delta}{k_z v_\delta})}{1 + i \sum_{m=-\infty}^{\infty} \Lambda_m(b_\delta) \frac{\nu_\delta}{k_z v_\delta} Z(\frac{\omega + i\nu_\delta - m\Omega_\delta}{k_z v_\delta})} . \tag{4}$$

In Eqs.(3) and (4) ω_{pe} and $\omega_{p\delta}$ are the plasma frequencies of electron and ion species δ, while v_e and v_δ are their thermal velocities, respectively. Ω_δ is the cyclotron frequency of the δ^{th} ion species, $\Lambda_m(b_\delta)$ is $I_m(b_\delta)\exp(-b_\delta)$, where I_m is the is the modified Bessel function of the order of m, $b_\delta = k_\perp^2 v_\delta^2/2\Omega_\delta^2$, $k_\perp$ is the perpendicular component of the wave number and k_z is the parallel wave number of the Bernstein wave with respect to the magnetic field. Z denotes the plasma dispersion function. For ions we include ion-ion collisions through a collisional damping decrement $\nu_\delta = b_\delta \nu_{ii}$ [1], where ν_{ii} is the ion-ion collisional frequency in the plasma.

For our purposes the susceptibilities in Eqs.(3) and (4) for the resonant Bernstein mode can be approximated as

$$\chi_e(\omega,\vec{k}) = -\frac{\omega_{pe}^2}{k^2 v_e^2}\frac{k_z^2 v_e^2}{\omega^2} , \quad \chi_\delta(\omega,\vec{k}) = \frac{\omega_{p\delta}^2}{k^2 v_\delta^2} \frac{1 - \frac{\omega + i\nu_\delta}{\omega + i\nu_\delta - m\Omega_\delta}\Lambda_m(b_\delta)}{1 - \frac{i\nu_\delta}{\omega + i\nu_\delta - m\Omega_\delta}\Lambda_m(b_\delta)} , \tag{5}$$

which are valid for $\Omega_\delta >> \omega - m\Omega_\delta >> k_z v_\delta$, $\omega >> k_z v_e$ and $\omega_{pe}^2/k^2 v_e^2 >> 1$. These conditions ensure a low cyclotron and electron Landau damping of the wave.

The resonant Bernstein mode is defined by the dispersion relation $\epsilon(\omega_B,\vec{k}_B) = 0$. The quasimode is strongly damped by electrons and/or ions, and its dielectric constant $\epsilon(\omega,\vec{k})$ deviates from zero.

The decay process can be described by coupled wave equations, which for the case of dipole approximation ($k_o = 0$) and electrostatic decay waves may be written as [1,6]

$$\{\epsilon(\omega_B,\vec{k}) + \sum_\delta \frac{\mu_\delta^2}{4} [\chi_\delta(\omega,\vec{k}) - 2\chi_\delta(\omega_B,\vec{k})]\} E_B = \sum_\delta \frac{\mu_\delta}{2} [\chi_\delta(\omega,\vec{k}) - \chi_\delta(\omega_B,\vec{k})] E, \quad (6a)$$

$$\{\epsilon(\omega,\vec{k}) + \sum_\delta \frac{\mu_\delta^2}{4} [\chi_\delta(\omega_B,\vec{k}) - 2\chi_\delta(\omega,\vec{k})]\} E = \sum_\delta \frac{\mu_\delta}{2} [\chi_\delta(\omega,\vec{k}) - \chi_\delta(\omega_B,\vec{k})] E_B, \quad (6b)$$

where the summation δ is over all species, including electrons. Only the wave equations for the Bernstein wave electric field E_B and the quasimode electric field E are considered because we assume a weak pump wave depletion (hence, the pump wave field E_o is nearly constant). Because of dipole approximation we have $\vec{k}_B = -\vec{k}$. The parameter $\mu_\delta = \vec{k}\cdot\vec{V}_\delta/\omega_o$ is the ratio of drift excursion to the wave length of the decay mode. It is given by [6]

$$\mu_\delta = \frac{q_\delta}{m_\delta} \frac{|\vec{k}\times\vec{E}_o|\Omega_\delta^2 - i\omega_o\Omega_\delta(\vec{k}\cdot\vec{E}_o)}{(\omega_o^2 - \Omega_\delta^2)\,\omega_o\Omega_\delta}, \quad (7)$$

where $\frac{1}{2}\vec{E}_o \exp(i\omega_o t)$ is the fast wave electric field. The decay fields E_B and E correspond to the phase dependence $E_B \propto \exp[i(\omega-\omega_o)t+i\vec{k}_B\cdot\vec{x}]$ and $E \propto \exp(i\omega t - i\vec{k}\cdot\vec{x})$. The contributions from other harmonics $\omega + m\omega_o$, $m = +1, \pm 2 \ldots$ are omitted. In deriving Eqs.(6a) and (6b) the weak coupling approximation $|\mu_\delta| < 1$ is used and thus higher order terms $\propto \mu_\delta^3, \mu_\delta^4 \ldots$ are not included. When both decay waves are resonant, i.e. $\epsilon(\omega,\vec{k}) = 0$ for both waves, it is possible to

drop the terms to $O(\mu_\delta^2)$ but for the non resonant case studied here the inclusion of the second term on the left-hand side of Eq.(6a) is necessary (the corresponding term in Eq.(6b) is written only for the sake of the symmetry) [7].

Inspection of Eq.(7) reveals that for the fast wave pump with a frequency in the ion cyclotron frequency range, both $\vec{E}x\vec{B}$-drift and polarization drift of ions may contribute to the instability. However, μ_δ for electrons is mainly determined by the $\vec{E}x\vec{B}$-drift of electrons unless $\vec{k}$ and $\vec{E}_o$ are parallel in which case μ_e is very small.

In the steady-state one is able to solve the nonresonant wave equation (6b) directly to have an adiabatic solution for the quasimode wave field

$$E = \frac{1}{\epsilon(\omega,\vec{k})} \sum_\delta \frac{\mu_\delta}{2} [\chi_\delta(\omega,\vec{k}) - \chi_\delta(\omega_B,\vec{k})]E_B, \tag{8}$$

where the terms of order μ_δ^2 are neglected. Using Eq.(8) one can eliminate E in Eq.(6a) and obtain a solution for convective amplification of E_B by expanding $\epsilon(\omega_B,\vec{k}) = \epsilon_R + i\epsilon_I$ as $\epsilon \approx i\epsilon_I + i(\partial\epsilon_R/\partial\vec{k})\cdot(\partial/\partial\vec{x})\ |\vec{k} = \vec{k}_B$. After some algebra one finds [6]

$$E_B = E_N \exp A \equiv$$

$$\equiv E_N \exp \{\int \frac{\sum_\delta \sum_\eta |\mu_\delta - \mu_\eta|^2 |\mathrm{Im}[\frac{\chi_\delta(\omega,\vec{k})\chi_\eta(\omega,\vec{k})}{\epsilon(\omega,\vec{k})}]| - \epsilon_I(\omega_B,\vec{k})}{8\ |\partial\epsilon_R(\omega_B,\vec{k})/\partial\vec{k}|_{\vec{k}=\vec{k}_B}} dx\}, \tag{9}$$

where E_N is the noise electric field, the summations δ and η are over all

species, Im{} denotes the imaginary part of the value in the brackets and x-integration is taken to be in the direction of the group velocity of the resonant Bernstein mode. $|\chi_\delta(\omega_B,\vec{k})| << |\chi_\delta(\omega,\vec{k})|$ is assumed to be valid for all species, which usually is a good approximation for the nonresonant decay, x-integration extends over the interaction region. The length of this region is determined from the finite pump wave extent or from any spatial extent over which the integrand has a non-negligible value, and from the frequency and wave number matching restrictions due to the plasma inhomogeneities. In a tokamak the radial (in the direction of minor radius) and poloidal extent is usually determined from the last two conditions while the parallel extent is determined from the finite pump wave extent.

In the earlier study [5] the threshold pump field was calculated for a exp(π) growth of E_B at the tokamak plasma edge. The lowest thresholds were found when the quasimode frequency and the Bernstein wave frequency are near any cyclotron harmonics of the ion species. The instability was also found to be strong only at sufficiently low temperature typical of the plasma edge. Because of the frequency matching condition a strong decay for a prescribed pump wave frequency is then expected only at definite magnetic field intervals. There is also a relatively narrow k_z-region over which A may have values larger than π. Note that k_{oz}, the parallel wave number of the pump wave, may be of the same order as k_z and has usually a broad spectrum. Hence, k_{Bz} of the resonant wave can deviate much from k_z of the quasimode and the threshold actually has to be minimised for k_z and k_{Bz} separately.

For H-minority heating of deuterium plasma in JET the decay of the fast wave to a hydrogen quasimode ($\omega \sim \Omega_H$) and deuterium Bernstein mode ($\omega_B \gtrsim \Omega_D$) in a scrape-off layer in front of the RF-antenna is possible. Due to the inverse major radius R^{-1} dependence of the magnetic field one should have the resonant layer [$\omega_o = \Omega_H(R)$] for the H-minority heating at radii R less than

3.0 m to satisfy the frequency matching for the instability at R = 4.15 m or less, corresponding to the scrape-off layer. Here, the possible paramagnetic correction to the R^{-1} dependence of the magnetic field has also been accounted. In a D-T-plasma the corresponding resonant layer should be at radii less than R = 3.1 m in order to have a strong decay to a hydrogen quasimode and to a tritium Bernstein mode (or a decay to a deuterium quasimode and a second harmonic tritium Bernstein mode at radii less than R = 3.4 m). Placing the resonance layer at larger radii or having a minority ion with a smaller cyclotron frequency (like He^3) would remove the possible interaction region of the parametric decay away from the tokamak plasma. In He^3-minority heating a possibility exists for the decay to majority ion quasimode and Bernstein mode (at the fundamental cyclotron frequencies) but this decay would have a fairly large threshold at any resonance layer location [5].

3. SATURATION MODEL

For any wave, the amplitude of the density fluctuation in the wave has to remain below the background density to avoid wave breaking. For the electrostatic waves one has in the linear regime the following relation between density fluctuation level and electric field

$$\left|\frac{\delta n_\delta}{n_\delta}\right| = \left|\frac{q_\delta}{m_\delta}\,\chi_\delta(\omega,\vec{k})\,\frac{k}{\omega_{p\delta}^2}\,E\right| , \qquad (10)$$

where δn_δ is the density fluctuation, n_δ is the background density of species δ and $|E|$ denotes the wave field amplitude. Using Eq.(5) for the susceptibilities, one obtains $E \sim 10^3$ V/cm, corresponding to 50% density fluctuations in a Bernstein wave with $k \sim 100$ cm^{-1}. Due to the wave breaking much larger wave fields are thus not possible. Nonlinearities like the parametric decay may suppress the wave field to an even lower value which is

probable because the parametric processes for the fast wave are already strong at the field level $E_o \sim 100$ V/cm. The Bernstein wave could decay to two other smaller frequency Bernstein modes or quasimodes, for instance. However, for the tritium Bernstein mode there is no obvious decay to lower frequency Bernstein waves due to the lack of ion species with lower ion cyclotron frequencies. The second harmonic generation [8] has to be ruled out for the Bernstein waves, because the second harmonic wave with a frequency and wave vector 2ω and $2\vec{k}$, respectively, is a non resonant and in most cases weakly damped mode. For the quasimode the decay is not possible but the coupling to another quasimode at second harmonic is possible. However, as E_B in Eq.(6a) is driven by the third order term which does not depend on E, saturation of the quasimode electric field will not affect the Bernstein wave. A conceivable secondary decay would then be the decay of the Bernstein mode E_B to another Bernstein mode E_B' with nearly the same frequency and to a low frequency electron quasimode E". Obviously the condition $\omega''/k_z'' v_e \sim 1$ should be satisfied for the beat frequency $\omega'' = \omega_B' - \omega_B$ and beat wave number $k_z'' = k_{Bz}' - k_{Bz}$ to have an electron quasimode at the beat frequency [here, ω_B' and k_{Bz}' are the frequency and the parallel wave number of the secondary Bernstein mode, respectively]. ω'' turns out to be typically much smaller than any ion cyclotron frequency.

In the following, we assume that the group velocities of the Bernstein modes are parallel to minimise the convective losses in the secondary decay. The coupling equations between the Bernstein modes E_B and E_B' may then be written as

$$\frac{\partial E_B}{\partial x} = \gamma E_B - \frac{B}{\partial \epsilon(\omega_B, k_B)/\partial k_B} |E_B'|^2 E_B \qquad (11)$$

$$\frac{\partial E_B'}{\partial x} = -\frac{\nu}{v_g'} E_B' + \frac{B}{\partial \epsilon(\omega_B', k_B')/\partial k_B'} |E_B|^2 E_B' \qquad (12)$$

where γ denotes the primary coupling strength and is given by the integrand in the exponential function in Eq.(9), ν is the collisional damping decrement of the secondary Bernstein wave and v_g' is the group velocity of that wave. The coupling coefficient B can be calculated (see the Appendix) from the expressions given [9] for the nonlinear Landau damping of the longitudinal waves in a magnetic field, and is

$$B = \{\frac{q}{M} \frac{2\omega_p^2}{k_B k_B' v_T^2} \frac{1}{v_T \Omega} \frac{p^2\Omega^2}{(\omega_B - p\Omega)(\omega_B' - p\Omega)} \int_0^\infty dx\, Y_{1,p} e^{-x^2}\}^2 \text{ Im } [\frac{1}{\epsilon(\omega'', k'')}] \ , \qquad (13)$$

where

$$Y_{1,p} = J_1(\frac{k'' v_T}{\Omega} x)\ J_p(\frac{k_B v_T}{\Omega} x)\ J_p(\frac{k_B' v_T}{\Omega} x) \ , \qquad (14)$$

with J_p denoting the Bessel function of the order of p, and Im [ ] denotes the imaginary part of the expression inside the brackets.

In deriving the coupling coefficient B we have assumed that $\omega_B - p\Omega$ and $\omega_B' - p\Omega$ are much smaller than Ω for a certain ion species and index p [q, M, v_T ω_p, and Ω denote the charge, mass, thermal velocity, plasma frequency and cyclotron frequency of that species]. If more than one ion species satisfy the previous conditions one has to sum the expression inside the square bracket in Eq.(13) over various species.

From Eq.(12) one obtains a threshold for the secondary decay which is defined by the collisional damping of E_B'

$$|E_B|^2 \geq \frac{\nu}{B} \partial \epsilon(\omega_B', k_B')/\partial \omega_B' \ . \qquad (15)$$

Provided that E_B can grow sufficiently to exceed this threshold, the equation system (11)-(12) leads to relaxation oscillations where the amplitudes of the two waves oscillate periodically in space [7,10]. The saturation level of the primary Bernstein wave is given by the maximum value of E_B. The equations (11) and (12) can be written for the energy densities using the relation $W = \epsilon_o \omega \, \partial\epsilon/\partial\omega \, E^2$, where W is the wave energy density and ϵ_o is the dielectric constant. Normalising the energy densities as

$$W = W_B/W_B(E_B = 100 \text{ V/cm}); \quad W' = \frac{v_g'}{v_g} \frac{\omega_B}{\omega_B'} W_B'/W_B(E_B = 100 \text{ V/cm}), \tag{16}$$

one can write Eqs.(11) and (12) as

$$\frac{\partial W}{\partial x} = 2\gamma W - \alpha W' W \tag{17}$$

$$\frac{\partial W'}{\partial x} = -\frac{2\nu}{v_g'} + \alpha W W', \tag{18}$$

where

$$\alpha = \frac{2B \cdot 10^4 [V^2/cm^2]}{\partial\epsilon(\omega_B', k_B')/\partial k_B'}. \tag{19}$$

These equations have the constant of motion

$$\alpha W - \frac{2\nu}{v_g'} \ln W = 2\gamma \ln W' - \alpha W' + c \, , \tag{20}$$

which gives c as a function of boundary values W_N and W_N' as

$$c = \alpha(W_N + W_N') - \frac{2\nu}{v_g'} \ln W_N - 2\gamma \ln W_N' \, . \tag{21}$$

W_M, the maximum value of W can be obtained by solving Eq.(17) for W' with the condition $\partial W/\partial x = 0$. Putting this W' then into Eq.(20) and using Eq.(21) gives us

$$\alpha W_M - \frac{2\nu}{v'_g} \ln \frac{W_M}{W_N} = 2\gamma \ln \frac{2\gamma}{\alpha W'_N} - 2\gamma \ , \tag{22}$$

where we have neglected $\alpha(W_N + W'_N)$ in c, because the noise values are typically very small. Eq.(22) can then be solved for W_M, which can be used to estimate the maximum power conversion in the primary fast wave decay.

Because of the Bernstein wave dispersion, the secondary Bernstein wave will have a larger wave number than the primary Bernstein wave and is then more strongly damped by collisions. It is obvious that this secondary decay broadens the primary Bernstein wave k spectrum to larger values, i.e. up to the collisional limit defined by the threshold of Eq.(15). We note that an essential part of the secondary Bernstein wave spectrum is not able to couple to the fast wave because of the higher collisional threshold and because of the frequency shift which does not allow any quasimode coupling back to the fast wave at the same spatial location. The excitation region of secondary Bernstein waves is also limited due to higher damping.

4. EVALUATION OF POWER CONVERSION

The amount of power converted in the fast wave decay can be estimated with the help of Eqs.(8) and (9) which determine the decay wave amplitudes at the steady-state. The power balance in the decay (neglecting the secondary decay for the time being) can be simply written as (assuming no linear damping of the fast wave)

$$P_{o\ in} - P_{o\ out} = P_B + P \ , \tag{23}$$

where $P_{o\ in}$ ($P_{o\ out}$) is the fast wave power coming into (going out of) the interaction region. P_B denotes the Bernstein wave power convecting out of the interaction region or being absorbed there. P is the power absorbed by the plasma particles through the quasimode. A special case is taken to illustrate the coupling geometry (see Fig.1). Here, the slab geometry is assumed. The fast wave propagates through the interaction region in the radial direction (x-direction). The extent of the interaction region in parallel direction (z-direction) is L and in the radial direction is D, while the poloidal extent is H. The fast wave power P_o coming in is evidently $W_o v_{go} HL$, where

$$W_o = 2\epsilon_o |E_{oy}|^2 \omega_{pi}^2/\Omega_i^2 \tag{24}$$

is the fast wave energy density in the plasma and $v_{go} \approx V_A \equiv \Omega_i c/\omega_{pi}$ is the group velocity of the fast wave. Similarly, P_B can be written as $W_B(L) V_{gB} DH$, where

$$W_B(L) = \epsilon_o |E_B(L)|^2 \frac{\omega_B}{\omega_B - \Omega_i} \frac{\omega_{pe}^2}{k^2 v_e^2} \tag{25}$$

is the amplified Bernstein wave energy density and $v_{gB} = 2(\omega_B - \Omega_i) k_z v_e^2/\omega_B^2$ is the group velocity of the Bernstein mode. Any absorption of power due to the Bernstein wave damping is omitted because our interest is in a well-amplified case, where $\epsilon_I(\omega_B, \vec{k})$ can be neglected in A in Eq.(9). From the Manley-Rowe relations of a three-wave interaction [7] the power P absorbed in the quasimode is simply $(\omega/\omega_B)P_B$. Hence, the power conversion factor describing the ratio of the power going into the decay waves and particles to that of the incoming pump power is

$$C \equiv \frac{P_B + P}{P_{o\ in}} = \frac{\omega_o}{\omega_B} \frac{v_{gB} W_B(L)}{v_{go} W_o} \frac{D}{L} \tag{26}$$

which can be easily calculated once the convective amplification A and, hence, $E_B(L)$ is determined. Note that Eq.(26) is applicable to other interaction geometries as well when one substitutes for D and L the lengths of the interaction geometry in the direction of the pump wave group velocity and Bernstein wave group velocity, respectively. For example, in the case when the Bernstein wave energy propagates in the x direction (small k_z), P_B is equal to $W_B(D)v_{gB}LH$ where v_{gB} is given by $(\omega_B - \Omega_i)/k$. Consequently the power conversion C is

$$C = \frac{\omega_o}{\omega_B} \frac{v_{gB}W_B(D)}{v_{go}W_o} . \tag{27}$$

The effect of the secondary decay can be introduced roughly by using the maximum Bernstein wave energy density W_M defined in Eq.(22) for $W_B(L)$ or for $W_B(D)$ in Eqs.(26) and (27). However, C will be much larger if the saturation amplitude is achieved at a shorter distance than L or D. To account for this effect and for the fact that the secondary decay is actually a many mode coupling system involving a broad spectrum of secondary waves, we adapt here a simple model in which the primary Bernstein wave grows to the saturation level, defined by W_M, with the growth rate of the primary instability and thereafter maintains a constant energy density W_M while propagating out of the interaction region. It is then possible to obtain from the wave equations describing the primary instability a power conversion from the fast wave, which is

$$C' = (1 + A - A_o)\, C. \tag{28}$$

Here C can be calculated from Eqs.(26) or (27), and A is defined in Eq.(9), while $A_o = \ell n\, E_M/E_N$ where E_M is defined as the maximum electric field

amplitude of the Bernstein wave calculated in the saturated model of Eq.(22). Hence, saturation as a function of the incoming fast wave power intensity is obtained but no saturation is found with respect to the interaction length or temperature, which, for instance, define A. However, power conversion is clearly strongly restrained with respect to the latter parameters by the secondary decay.

5. CALCULATIONS

5.1 The Threshold of the Instability

In the following examples the quasimode frequency is chosen to be the hydrogen cyclotron frequency (fundamental). The coupling was shown [5] to be strongest for that particular case because deuterium (as well as tritium) ions resonate at that frequency and $\mathrm{Im}\{\chi_D\chi_H/\epsilon\}$ in A (see Eq.(9)) becomes large. In the hydrogen minority heating of a deuterium plasma the decay to the hydrogen quasimode ($\omega \sim \Omega_H$) and deuterium Bernstein mode could be possible in JET provided the resonance layer ($\omega_o = \Omega_H(R)$) for ion cyclotron heating lies in the inner side of the torus ($R \lesssim 3.0$ m). In D-T plasma the decay to the hydrogen quasimode and tritium Bernstein mode would exist if the resonance layer were located at major radii less than R = 3.1 m.

In the following calculations the center value of the magnetic field is taken to be B = 3.15 T. This corresponds to the edge value of the magnetic field B = 2.24 T at R = 4.15 m. The edge temperature T is taken to be 50 eV for electrons and ions, while the edge electron density n_e is taken to be 4.75×10^{18} m^{-3}.

As the first example we study the decay to the hydrogen quasimode and the deuterium Bernstein mode in a deuterium-hydrogen plasma. Choosing f_o = 52.84 MHz for the pump wave frequency, one has $\omega_B = 1.094\ \Omega_D$ and k = 93 cm^{-1} for the Bernstein wave. The maximum for A is obtained at a specific k_z for the

quasimode once the geometry of the interaction region is defined. Here, we assume that the parallel wave number k_{oz} of the pump wave has a narrow peak at zero. Hence, $k_z \sim -k_{Bz}$ should be well satisfied for the decay waves. The optimum Bernstein perpendicular wave number direction is obviously poloidal because in radial direction the interaction region is limited by the quasimode condition $\omega - \Omega_H \lesssim k_z v_H$ under the spatial variation of Ω_H. This gives $d = 2Rk_z v_H/\Omega_H$ for the width d of the interaction region in the radial direction. Here the instability is driven mainly by the relative drift of deuterium and hydrogen ions, and $\mathrm{Im}\{\chi_D\chi_H/\epsilon\}$ in Eq.(9) is maximised for relatively low values of k_z less than 0.02 cm^{-1}. Hence, d is only a few millimetres for the chosen parameters and radial convection would be very rapid. To see that the instability is mainly driven by the relative drift of ions one has to note that $\mathrm{Im}\{\chi_e\chi_D/\epsilon\}$ or $\mathrm{Im}\{\chi_e\chi_H/\epsilon\}$ is maximised for relatively large values of k_z of the order of 0.2 cm^{-1}. Large k_z leads to a very large parallel group velocity of the Bernstein mode (note $|k_{Bz}| = |k_z|$) with an excessive parallel convective damping.

The widths of the interaction region in parallel and poloidal directions have the upper limits determined by the finite extent of the pump wave. We take L = H = 50 cm for the upper limits in the parallel (L) and poloidal (H) directions. However, a more stringent limit may come from the radial component of the Bernstein wave group velocity which may cause a more rapid convection than the parallel and poloidal components. Note that the radial component will develop even if one initially assumes no radial wave number component. This is due to the effect of radial inhomogeneities on the ray propagation. A simple calculation gives $L = 2(4L_T d)^{1/2} v_{gz}/v_{gy}$ and $H = 2(4L_T d)^{1/2}$, where $L_T (\gg d)$ is the local gradient scale length of the temperature, which is the most important source of inhomogeneity. In the following we take L_T = 3 cm.

The Landau and cyclotron damping of the Bernstein mode proves to be

negligible for the optimum k_z ($\sim$ 0.01 cm^{-1}). However, ion collisional damping limits the attainable perpendicular wave number which has a fairly strict upper limit given by $kv_D/\Omega_D \sim 5$ with the assumed temperature.

At k_z = 0.01 cm^{-1} and 5% hydrogen concentration the decay has a threshold electric field E_o = 45 V/cm (A = π). With k_z = 0.01 cm^{-1} we get d $\sim$ 3.8 mm, $v_{gz}/v_{gy} \sim 10$, L = 43 cm, and H $\sim$ 4.3 cm defining the dimensions of the interaction region. Pump wave electric field was assumed to be in the poloidal direction. As is evident from Eq.(7) this assumption does not have significant effect on the threshold.

As a second example we assume a D-T-H plasma with concentrations 47.5%, 47.5% and 5% for deuterium, tritium and hydrogen, respectively. The decay to the hydrogen quasimode and the tritium Bernstein mode has a threshold field E_o = 49 V/cm at k_z = 0.01 cm^{-1}. Again the instability is driven by the relative drift of ions, and the amplification is maximised for relatively low k_z. Here again d = 3.8 mm, H = 4.3 cm, but as $v_{gz}/v_{gy} \sim 20$, L = 50 cm. The Bernstein wave frequency ω_B is near the tritium cyclotron frequency, i.e. $\omega_B - \Omega_T$ = 0.045 Ω_T which gives k = 72 cm^{-1} and f_o = 46.05 MHz. At smaller k_z the thresholds are smaller but the radial extent d of the interaction region may become so small that a well defined Bernstein mode may not exist (for comparison, the perpendicular wave length of the Bernstein mode is about 0.6 mm). At larger k_z the coupling decreases and the parallel convective damping increases the threshold.

Diminishing $\omega_B - \Omega_T$ (or $\omega_B - \Omega_D$ in the previous example) implies stronger coupling via the increase of k but the condition $k\lambda_{De} < 1$, where λ_{De} is the Debye length, for the existence of weakly damped electrostatic Bernstein modes may be violated. Also the increasing collisional damping will make the thresholds higher at larger k. At smaller temperatures or smaller magnetic fields the thresholds become lower due to the increase of k at constant $\omega_B - \Omega_T$ (or $\omega_B - \Omega_D$). For example, with T = 30 eV (k_z = 0.013 cm^{-1}, k = 93 cm^{-1})

one obtains E_o = 40 V/cm for the decay to the hydrogen quasimode and tritium Bernstein mode. At still lower temperatures the collisional damping begins to dominate the convective damping and the threshold stops decreasing. At higher temperatures the threshold increases as $E_o \propto T^{3/4}$. In Fig.2 we plot the amplification factor A vs. temperature T for different pump electric fields. For low temperatures (< 100 eV) A increases with decreasing T, while for higher temperatures (> 100 eV) it decreases roughly as $T^{-3/2}$. The dependence on the magnetic field is roughly $E_o \propto B^{-1/2}$ (no collisional damping) as is evident from Eqs.(7) and (9). The increase of hydrogen concentration n_H lowers the thresholds as $E_o \propto (n_H)^{-1/2}$, which is valid in the range $2\% \lesssim n_H \lesssim 15\%$.

5.2 Power Conversion

To calculate the power conversion factor from Eqs.(26) and (28) one has to determine the dimensions L and D. Because $v_{gz} >> v_{gy}$ is valid for the Bernstein wave group velocities in the previous examples, the geometry of Fig.1 is applicable to the present case. L is taken to be the width of the RF antenna which is 50 cm. D can be estimated from the temperature dependence of the threshold field. This being relatively weak between 25 eV and 75 eV we choose D = 3 cm corresponding to the main part of the scrape-off layer of JET plasma. In calculating A the values T = 50 eV and $n = 4.75 \times 10^{18}$ m^{-3} will be used. The magnetic field is 2.24 T at R = 4.15 m, as previously, and the pump wave electric field is assumed to be 100 V/cm. In the deuterium plasma the corresponding A is then 22.6 and in the deuterium-tritium plasma one gets A = 21.0 with the parameters of the previous section. Assuming a noise field $E_N \sim 10^{-6}$ V/cm for the Bernstein waves in the unstable $\vec{k}$-spectrum, one obtains the amplified field level $E_N \exp A = 6.4 \times 10^3$ V/cm and 1.3×10^3 V/cm for the

deuterium Bernstein mode and tritium Bernstein mode, respectively. We see that the obtained amplified Bernstein wave fields are of the same order as the wave breaking limit $E_B = 10^3$ V/cm from Eq.(10). Using this saturation level in Eq.(26) one obtains for the case of the deuterium Bernstein wave, a power conversion factor $C \sim 0.025$ with the power influx 3 MW/m² of the fast wave. Assuming an area of 0.5 m² for the antenna, the power absorbed by the parametric instability per antenna amounts to about 40 kW in the scrape-off layer. For the tritium Bernstein wave case $C \sim 0.06$, the power absorbed per antenna is about 90 kW.

To consider the effect of the secondary decay we have to calculate B of Eq.(13). We concentrate only on the tritium Bernstein wave case and take $\omega_B' - \Omega_T = 0.0225\ \Omega_T$ which gives $k_B' = 137$ cm^{-1} and $k'' = -65$ cm^{-1} for the electron quasimode. The parallel wave numbers are chosen to be 0.006 cm^{-1} and 0.004 cm^{-1} for the secondary Bernstein wave and the quasimode, respectively. With these parameters the quasimode is strongly damped on electrons and we have $\epsilon(\omega'',k'') \approx 49 + i29$. The group velocities of the Bernstein waves are also nearly parallel and predominantly in the z-direction. B turns out to be for tritium species with p = 1 equal to 1.65×10^{-3} cm²/V². From Eq.(15) one then obtains a collisional threshold $E_B \sim 20$ V/cm. α from Eq.(19) is 26.5 cm^{-1}, where we have used the z-component of $\partial\epsilon(\omega_B', \vec{k}_B')/\partial\vec{k}_B'$. Similarly $2\upsilon/v_{gz}' \approx 1.1$ cm^{-1}. With $E_o = 100$ V/cm, A is 21, and 2γ, consequently, is 0.84 cm^{-1} with L = 50 cm. Assuming $E_N = E_N' = 10^{-6}$ V/cm for the Bernstein wave field noises, one finds from Eq.(22) $W_M = 2.6$ which corresponds to a saturation amplitude $E_B \approx 160$ V/cm. The amplification factor A_o needed to reach this value is about 19, and from Eqs.(26) and (28) one gets $C' \sim 0.0046$ with the power influx 3 MW/m² of the fast wave, and C computed with $E_B(L) = 160$ V/cm. For the deuterium Bernstein wave case, a somewhat smaller power conversion is obtained. Hence, only a few kilowatts or less is absorbed by the fast wave

decay per antenna in our examples if the secondary decay process presented in this paper can operate. The result is not very sensitive to the noise levels assumed but depends strongly on the collisional damping decrement assumed.

6. DISCUSSION

Edge absorption of RF power by a non resonant parametric decay of the fast wave in the ICRF heating of a JET plasma is estimated. It is shown that at a relatively low fast wave electric field level 100 V/cm, the decay to hydrogen quasimode and the deuterium or tritium Bernstein mode may be easily observed at the plasma edge. In a deuterium plasma the decay would be possibly present in a non optimal heating case where the ion cyclotron resonance layer for hydrogen minority heating is located in the inner side of the torus at major radii less than 3.0 m. In the deuterium-tritium plasma the decay would be possible with typical heating conditions where the resonance layer for the hydrogen minority (or deuterium second harmonic) heating is located at major radii less than 3.1 m.

The power conversion depends sensitively on the fast wave electric field E_o, the decay interaction geometry and on some plasma parameters. The power going into the Bernstein wave energy in the linear phase of the instability is proportional to exp(2A) where A is defined in Eq.(9). Because A is roughly proportional to $|E_o|^2$ the power conversion is sensitive to E_o. For instance, with E_o = 80 V/cm instead of 100 V/cm in our examples, the converted power would have been less than 10^{-6} times the obtained value and hence negligible. The dependence of the power conversion on the Bernstein wave noise level E_N is $C \propto E_N^2$ (from Eqs.(9) and (26)) and therefore affects the result strongly. These dependences, of course, do not hold when the Bernstein wave field amplitude approaches and exceeds the nonlinear saturation level. This was assumed to be of the order of 10^2 V/cm in this paper. At larger fields the ion density fluctuations approach the background density and it is shown that

a secondary decay of the Bernstein wave to another Bernstein wave and an electron quasimode may quench or restrain the growth of the instability. The results of this paper indicate that this nonlinear regime can be achieved with pump fields of about 100 V/cm in JET. The secondary decay restricts the power conversion to a few kilowatts for power influx of 3 MW/m² which is typical of JET ICRH heating scenarios.

The exponential growth factor A is also sensitive to the plasma temperature, magnetic field and the hydrogen concentration, while there is no strong dependence on electron density [5]. Roughly, a dependence $A \sim T^{-3/2}B^{-1}n_H$ may be derived from Eq.(9) for an optimum growth (collisional damping neglected). According to this, larger amplification may be obtained at lower temperatures and weaker magnetic fields. The radial width D of the interaction region was based on this dependence which may imply an error in C by a factor of about 2. However, noting the extreme sensitivity of the power conversion factor to E_o, such errors in defining C are admissable in Eq.(26). The accuracy of the estimates presented in this paper depends mostly on the accuracy in obtaining A and in defining the nonlinear saturation limit for the Bernstein wave amplitude. Therefore, more detailed calculations should be made to assess the Bernstein wave ray trajectory in the interaction region where the inhomogeneities as well as any possible magnetic noise should be known precisely. Any broadening of the fast wave number (or frequency) spectrum would evidently decrease A [11]. For instance, if the fast wave has a spectral width Δk_{oz} in parallel wave number, the previously obtained A should be multiplied by $\delta k_z/\Delta k_{oz}$, where δk_z is the characteristic width of the unstable quasimode spectrum in parallel wave number.

According to the results presented in this paper, the secondary decay of the Bernstein wave could restrict the electric field level of the Bernstein wave at the same level as that of fast wave electric field. Because of the

slow group velocity of the Bernstein wave as compared to the fast wave group velocity, the power conversion would remain negligible in the coupling geometries studied in this paper. We note that the present saturation mechanism should be applicable to any non-resonant or resonant Bernstein wave decay of the fast wave. Further consideration should evidently be given for the full spectrum of the secondary decay wave as well as for the effect of the width in the primary Bernstein wave spectrum, which, in turn, may weaken the secondary decay process.

ACKNOWLEDGEMENTS

It is a pleasure to thank Drs. T. Hellsten and W. Core and Mr. G. Devillers for many valuable discussions in the course of this work.

The authors wish to thank Mr. C.M. Farrell for his assistance with the programming and computations.

J.A. Heikkinen would also like to thank the Theory Division for hospitality, and the Finnish Cultural Foundation and Imatran Voima Foundation for financial support.

APPENDIX

Coupling Equations in the Secondary Decay

Our starting point is the three-wave equation system [9]

$$\frac{\partial E_B}{\partial x} = - \sum_j \frac{H}{\partial \epsilon(\omega_B, k_B)/\partial k} E'_B E''^* \tag{A1}$$

$$\frac{\partial E'_B}{\partial x} = \sum_j \frac{H}{\partial \epsilon(\omega'_B, k'_B)/\partial k} E_B E'' \tag{A2}$$

$$E'' = - i \sum_j \frac{H}{\epsilon(\omega'', k'')} E^*_B E'_B \tag{A3}$$

which describes the nonlinear electron Landau damping of the Bernstein wave field E_B. The frequency and wave number matching conditions $\omega'' = \omega'_B - \omega_B$, $\vec{k}'' = \vec{k}'_B - \vec{k}_B$, respectively, are assumed with a definition

$$E_B(x,t) = E_B \exp\left[i(\vec{k}_B \cdot \vec{x} - \omega_B t)\right] + E^*_B \exp\left[-i(\vec{k}_B \cdot \vec{x} - \omega_B t)\right] \tag{A4}$$

valid for E_B, and similarly for the other waves. The interaction coefficient H is given by

$$H = \frac{q\omega_p^2}{k_B k'_B k'' M} \sum_{s,\ell} \int_{-\infty}^{\infty} dv_z \int_0^{\infty} dv_\perp v_\perp \, Y_{\ell,s} \, k'_B \frac{k'' Z_{s-\ell}(k) + k_B Z_\ell(k'')}{(\omega'_B - s\Omega - k'_{Bz} v_z)^2 - \Omega^2} , \tag{A5}$$

where q and M are the charge and mass of the j^{th} species with ω_p denoting the corresponding plasma frequency. $Y_{\ell,s}$ is defined by

$$Y_{\ell,s} = J_\ell(k''v_\perp/\Omega)\ J_{s-\ell}(k_B v_\perp/\Omega)\ J_s(k_B' v_\perp/\Omega)\ , \tag{A6}$$

where J_ℓ, for instance, is the Bessel function of order ℓ. Z_n is defined by

$$Z_n(k) = \frac{(n\Omega/v_\perp)\partial F_o/\partial v_\perp + k_z \partial F_o/\partial v_z}{\omega - n\Omega - k_z v_z}\ , \tag{A7}$$

where F_o is the background distribution function (for j^{th} species). In the expression for H we have neglected terms which are smaller by a factor of k_z^2/k^2 and the total wave number is used for the perpendicular wave number.

The equations (A1-A3) reduce readily to those of Eqs.(11) and (12) if one eliminates E" from Eqs.(A1) and (A2) with the help of Eq.(A3). The interaction coefficient B is then

$$B = [\sum_j H]^2 \quad \mathrm{Im}[\frac{1}{\epsilon(\omega'',k'')}]\ , \tag{A8}$$

where Im[ ] denotes the imaginary part of the expression inside the brackets.

The third order corrections have been neglected in Eqs.(A1-A3) because we have assumed that the quasimode is damped only by electrons for which case the third order term can be shown to be negligible in the assumed coupling geometry ($\vec{k}' \times \vec{E}_B = 0$). This can be seen directly from Eqs.(6a), (6b) and (7) which are valid for electrons with some algebraical corrections coming from the finite pump wave number. From the same reason, H computed for electrons turns out to be negligible, which in fact has allowed us to place the square of $\sum_j H$ outside of the imaginary operator Im in Eq.(A8). The summation over j here is meant only to include the ions.

To compute H we assume that $\omega_B - p\Omega$ and $\omega_B' - p\Omega$ are much smaller than Ω for some ion species and index p. Consequently, ω'' is much less than Ω and

the quasimode has a negligible ion cyclotron damping. Similarly, $\omega_B - p\Omega >> k_{Bz}v_z$ and $\omega'_B - p\Omega >> k'_{Bz}v_z$ are valid. Hence, we can approximate H for that particular ion species as

$$H = \frac{q\omega_p^2}{k_B k'_B k'' M} \int_{-\infty}^{\infty} dv_z \int_o^{\infty} dv_\perp v_\perp \{[\sum_s Y_{o,s}(k'' \frac{s\Omega}{\omega_B - s\Omega} + k_B \frac{k''v_z}{\omega'' - k''v_z})$$

$$+ \sum_{\substack{s,r \\ s\neq r}} Y_{s-r,s} (k'' \frac{r\Omega}{\omega_B - r\Omega} - k_B)] \frac{k'_B}{(\omega'_B - s\Omega)^2 - \Omega^2}\}[-\frac{4}{v_T^5}\pi^{-3/2}\exp(-v^2/v_T^2)], \quad (A9)$$

where we have introduced a Maxwellian distribution for F_o. We now pick up the largest terms from the sum which evidently are in the second part inside the square brackets with r = p and s = p±1. Using the Bessel function identity $(2p/x)J_p(x) = J_{p+1}(x) + J_{p-1}(x)$ one obtains from Eq.(A9)

$$H \approx \frac{q}{M} \frac{4\omega_p^2}{k_B k'_B v_T^2} \frac{1}{v_T\Omega} \frac{p^2\Omega^2}{(\omega_B - p\Omega)(\omega'_B - p\Omega)} \int_o^{\infty} dx\, Y_{1,p} e^{-x^2}, \quad (A10)$$

where

$$Y_{1,p} = J_1(\frac{k''v_T}{\Omega} x)\ J_p(\frac{k_B v_T}{\Omega} x)\ J_p(\frac{k'_B v_T}{\Omega} x)\ . \quad (A11)$$

For other ion species, H is evidently much smaller and is neglected. We note that in the dipole approximation limit ($|k_B| << |k'_B|, |k''|$) the integral in Eq.(A10) simplifies and one readily obtains the coupling coefficients on the right hand side of Eqs.(6a) and (6b) from Eqs.(A2) and (A3) within the approximations used. However, note that the electric fields in this Appendix have to be multiplied by a factor 2 to obtain the electric fields defined in Eqs.(6a) and (6b) because of the different definitions used. Noting this and using Eqs.(A8) and (A10) one obtains the coupling coefficient of Eq.(13).

REFERENCES

[1] HARMS, K.D., HASSELBERG, G. and ROGISTER, A. "Parametric excitation of ion Bernstein waves in a plasma with two ion species", Nucl. Fusion 14 (1974) 657.

[2] SKIFF, F., ONO, M. and WONG, K.L. "Parametric excitation of ion Bernstein waves by a fast wave antenna in the ion cyclotron frequency range", Phys. Fluids 27 (1984) 1051.

[3] SHARMA, O.P., TRIPATHI, V.K. and LIU, C.S. "Decay instability of an ion-cyclotron wave in a plasma", Phys. Fluids 25 (1982) 1598.

[4] Van NIEUWENHOVE, R., Van OOST, G., NOTERDAEME, J.M., BRAMBILLA, M., GERNHARDT, J. and PORKOLAB, M. "Parametric decay in the edge plasma of ASDEX during fast wave heating in the ion cyclotron frequency range", Nucl. Fusion 28 (1988) 1603.

[5] AVINASH, K., CORE, W.G.F. and HELLSTEN, T. "The nonlinear decay of the fast wave during ICRF heating". Presented at 2nd Int. Conf. on Plasma edge theory, 26-30 April 1988, Augustusburg, to appear in Contr. Plasma Phys.

[6] ONO, M., PORKOLAB, M. and CHANG, R.P.H. "Parametric decay into ion cyclotron waves and drift waves in multi-ion species plasma", Phys. Fluids 23 (1980) 1656.

[7] HASEGAWA, A. "Plasma instabilities and nonlinear effects", Physics and Chemistry in Space, Vol.8, Springer-Verlag, 1975.

[8] HEIKKINEN, J.A. and KARTTUNEN, S.J. "Saturation of parametric instabilities in lower hybrid heating of tokamak plasmas", Nucl. Fusion 27 (1987) 135.

[9] PORKOLAB, M. and CHANG, R.P.H. "Instabilities and induced scattering due to nonlinear Landau damping of longitudinal plasma waves in a magnetic field", Phys. Fluids 15 (1972) 283.

[10] WHITE, R.B., LEE, Y.C. and NISHIKAWA, K. "Nonlinear mode coupling and relaxation oscillations", Phys. Rev. Lett. 29 (1972) 1315.

[11] VALEO, E.J. and OBERMAN, C.R. "Excitation by an imperfect pump", Phys. Rev. Lett. 30 (1973) 1035.

[12] Van NIEUWENHOVE, R., Van OOST, G., BEUKEN, J.M., De KEYSER, L., DELVIGNE, T., DESCAMPS, P., DURODIE, F., GAIGNEAUX, M., JADOUL, M., KOCH, R., LEBAU, D., MESSIAEN, A.M., ONGENA, J., SHEN, X.M., VANDENPLAS, P.E., Van WASSENHOVE, G., WEYNANTS, R.R. In Proc. 15th Euro. Conf. on Controlled Fusion and Plasma Heating, Dubrovnik, May 16-20, 1988 Contributed papers Part II, pp.778.

[13] BURES, M., AVINASH, K., BRINKSCHULTE, H., DEVILLERS, G., JACQUINOT, J., KNOWLTON, S., POCHELON, A., START, D. and TAGLE, J. "RF edge field behaviour and parametric decay during ICRF heating on JET", Am. Phys. Soc. Bull. 33 (1988) 2032.

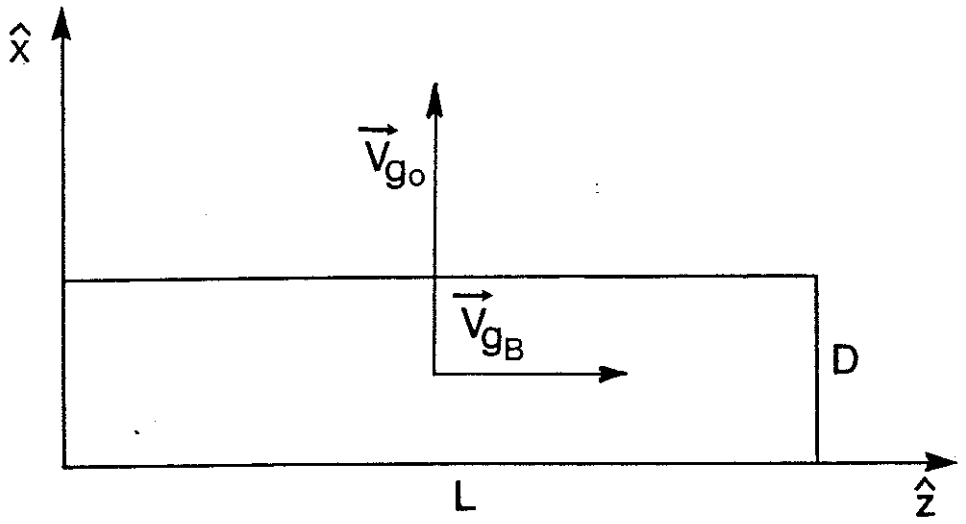

Fig.1 Directions of the group velocities of the fast wave ($\vec{v}_{go}$) and the Bernstein wave ($\vec{v}_{gB}$) inside the coupling region having a length D in radial direction (x) and L in parallel direction (z). The Bernstein wave has also a group velocity component in poloidal direction (y) which is not shown. The magnitude of the group velocity of the Bernstein wave is much smaller (10^{-2} - 10^{-3} times) as compared to the magnitude of the fast wave group velocity.

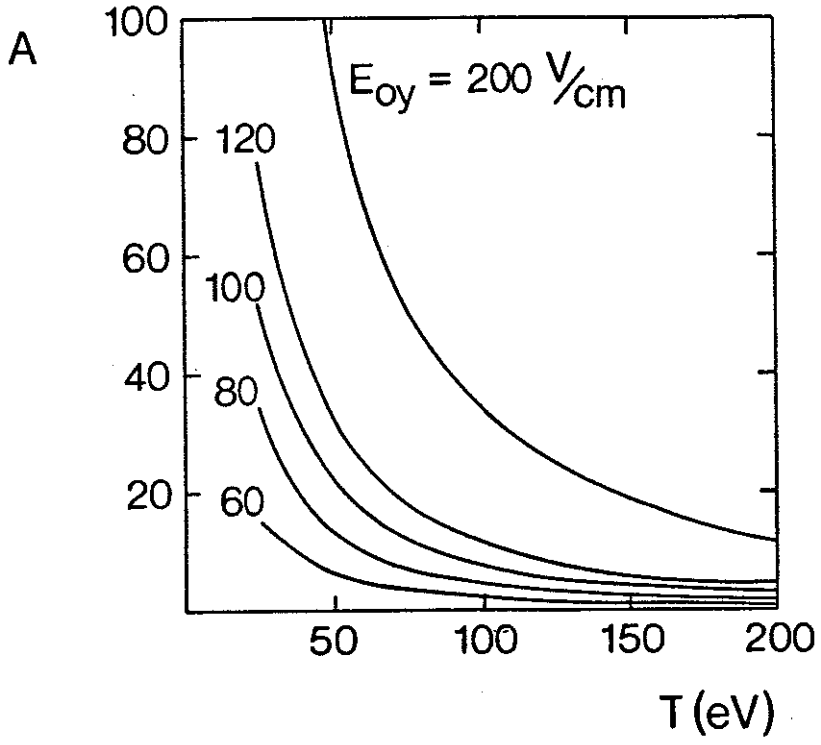

Fig.2 Exponential amplification factor A computed as a function of temperature T and fast wave electric field E_{oy} for the fast wave decay to the tritium Bernstein wave ($\omega_B \sim \Omega_T$) and the hydrogen quasimode ($\omega \sim \Omega_H$). 5% hydrogen concentration with equal amounts of deuterium and tritium is assumed. The parameters are: f_o = 46.05 MHz, k = 72 cm^{-1}, k_z = 0.01 cm^{-1}, L = 50 cm, B = 2.24 T and n_e = 4.75x10^{18} m^{-3}.

APPENDIX 1.

THE JET TEAM

JET Joint Undertaking, Abingdon, Oxon, OX14 3EA, U.K.

J.M.Adams[1], F.Alladio[4], H.Altmann, R.J.Anderson, G.Appruzzese, W.Bailey, B.Balet, D.V.Bartlett, L.R.Baylor[24], K.Behringer, A.C.Bell, P.Bertoldi, E.Bertolini, V.Bhatnagar, R.J.Bickerton, A.Boileau[3], T.Bonicelli, S.J.Booth, G.Bosia, M.Botman, D.Boyd[31], H.Brelen, H.Brinkschulte, M.Brusati, T.Budd, M.Bures, T.Businaro[4], H.Buttgereit, D.Cacaut, C.Caldwell-Nichols, D.J.Campbell, P.Card, J.Carwardine, G.Celentano, P.Chabert[27], C.D.Challis, A.Cheetham, J.Christiansen, C.Christodoulopoulos, P.Chuilon, R.Claesen, S.Clement[30], J.P.Coad, P.Colestock[6], S.Conroy[13], M.Cooke, S.Cooper, J.G.Cordey, W.Core, S.Corti, A.E.Costley, G.Cottrell, M.Cox[7], P.Cripwell[13], F.Crisanti[4], D.Cross, H.de Blank[16], J.de Haas[16], L.de Kock, E.Deksnis, G.B.Denne, G.Deschamps, G.Devillars, K.J.Dietz, J.Dobbing, S.E.Dorling, P.G.Doyle, D.F.Düchs, H.Duquenoy, A.Edwards, J.Ehrenberg[14], T.Elevant[12], W.Engelhardt, S.K.Erents[7], L.G.Eriksonn[5], M.Evrard[2], H.Falter, D.Flory, M.Forrest[7], C.Froger, K.Fullard, M.Gadeberg[11], A.Galetsas, R.Galvao[8], A.Gibson, R.D.Gill, A.Gondhalekar, C.Gordon, G.Gorini, C.Gormezano, N.A.Gottardi, C.Gowers, B.J.Green, F.S.Griph, M.Gryzinski[26], R.Haange, G.Hammett[6], W.Han[9], C.J.Hancock, P.J.Harbour, N.C.Hawkes[7], P.Haynes[7], T.Hellsten, J.L.Hemmerich, R.Hemsworth, R.F.Herzog, K.Hirsch[14], J.Hoekzema, W.A.Houlberg[24], J.How, M.Huart, A.Hubbard, T.P.Hughes[32], M.Hugon, M.Huguet, J.Jacquinot, O.N.Jarvis, T.C.Jernigan[24], E.Joffrin, E.M.Jones, L.P.D.F.Jones, T.T.C.Jones, J.Källne, A.Kaye, B.E.Keen, M.Keilhacker, G.J.Kelly, A.Khare[15], S.Knowlton, A.Konstantellos, M.Kovanen[21], P.Kupschus, P.Lallia, J.R.Last, L.Lauro-Taroni, M.Laux[33], K.Lawson[7], E.Lazzaro, M.Lennholm, X.Litaudon, P.Lomas, M.Lorentz-Gottardi[2], C.Lowry, G.Magyar, D.Maisonnier, M.Malacarne, V.Marchese, P.Massmann, L.McCarthy[28], G.McCracken[7], P.Mendonca, P.Meriguet, P.Micozzi[4], S.F.Mills, P.Millward, S.L.Milora[24], A.Moissonnier, P.L.Mondino, D.Moreau[17], P.Morgan, H.Morsi[14], G.Murphy, M.F.Nave, M.Newman, L.Nickesson, P.Nielsen, P.Noll, W.Obert, D.O'Brien, J.O'Rourke, M.G.Pacco-Düchs, M.Pain, S.Papastergiou, D.Pasini[20], M.Paume[27], N.Peacock[7], D.Pearson[13], F.Pegoraro, M.Pick, S.Pitcher[7], J.Plancoulaine, J-P.Poffé, F.Porcelli, R.Prentice, T.Raimondi, J.Ramette[17], J.M.Rax[27], C.Raymond, P-H.Rebut, J.Removille, F.Rimini, D.Robinson[7], A.Rolfe, R.T.Ross, L.Rossi, G.Rupprecht[14], R.Rushton, P.Rutter, H.C.Sack, G.Sadler, N.Salmon[13], H.Salzmann[14], A.Santagiustina, D.Schissel[25], P.H.Schild, M.Schmid, G.Schmidt[6], R.L.Shaw, A.Sibley, R.Simonini, J.Sips[16], P.Smeulders, J.Snipes, S.Sommers, L.Sonnerup, K.Sonnenberg, M.Stamp, P.Stangeby[19], D.Start, C.A.Steed, D.Stork, P.E.Stott, T.E.Stringer, D.Stubberfield, T.Sugie[18], D.Summers, H.Summers[20], J.Taboda-Duarte[22], J.Tagle[30], H.Tamnen, A.Tanga, A.Taroni, C.Tebaldi[23], A.Tesini, P.R.Thomas, E.Thompson, K.Thomsen[11], P.Trevalion, M.Tschudin, B.Tubbing, K.Uchino[29], E.Usselmann, H.van der Beken, M.von Hellermann, T.Wade, C.Walker, B.A.Wallander, M.Walravens, K.Walter, D.Ward, M.L.Watkins, J.Wesson, D.H.Wheeler, J.Wilks, U.Willen[12], D.Wilson, T.Winkel, C.Woodward, M.Wykes, I.D.Young, L.Zannelli, M.Zarnstorff[6], D.Zasche[14], J.W.Zwart.

PERMANENT ADDRESS

1. UKAEA, Harwell, Oxon. UK.
2. EUR-EB Association, LPP-ERM/KMS, B-1040 Brussels, Belgium.
3. Institute National des Récherches Scientifique, Quebec, Canada.
4. ENEA-CENTRO Di Frascati, I-00044 Frascati, Roma, Italy.
5. Chalmers University of Technology, Göteborg, Sweden.
6. Princeton Plasma Physics Laboratory, New Jersey, USA.
7. UKAEA Culham Laboratory, Abingdon, Oxon. UK.
8. Plasma Physics Laboratory, Space Research Institute, Sao José dos Campos, Brazil.
9. Institute of Mathematics, University of Oxford, UK.
10. CRPP/EPFL, 21 Avenue des Bains, CH-1007 Lausanne, Switzerland.
11. Risø National Laboratory, DK-4000 Roskilde, Denmark.
12. Swedish Energy Research Commission, S-10072 Stockholm, Sweden.
13. Imperial College of Science and Technology, University of London, UK.
14. Max Planck Institut für Plasmaphysik, D-8046 Garching bei München, FRG.
15. Institute for Plasma Research, Gandhinagar Bhat Gujat, India.
16. FOM Instituut voor Plasmafysica, 3430 Be Nieuwegein, The Netherlands.
17. Commissiariat à L'Energie Atomique, F-92260 Fontenay-aux-Roses, France.
18. JAERI, Tokai Research Establishment, Tokai-Mura, Naka-Gun, Japan.
19. Institute for Aerospace Studies, University of Toronto, Downsview, Ontario, Canada.
20. University of Strathclyde, Glasgow, G4 ONG, U.K.
21. Nuclear Engineering Laboratory, Lapeenranta University, Finland.
22. JNICT, Lisboa, Portugal.
23. Department of Mathematics, Univeristy of Bologna, Italy.
24. Oak Ridge National Laboratory, Oak Ridge, Tenn., USA.
25. G.A. Technologies, San Diego, California, USA.
26. Institute for Nuclear Studies, Swierk, Poland.
27. Commissiariat à l'Energie Atomique, Cadarache, France.
28. School of Physical Sciences, Flinders University of South Australia, South Australia SO42.
29. Kyushi University, Kasagu Fukuoka, Japan.
30. Centro de Investigaciones Energeticas Medioambientales y Techalogicas, Spain.
31. University of Maryland, College Park, Maryland, USA.
32. University of Essex, Colchester, UK.
33. Akademie de Wissenschaften, Berlin, DDR.

CR 88.49.1A